

This discussion paper is/has been under review for the journal Ocean Science (OS).  
Please refer to the corresponding final paper in OS if available.

# An automated gas exchange tank for determining gas transfer velocities in natural seawater samples

K. Schneider-Zapp<sup>1</sup>, M. E. Salter<sup>2</sup>, and R. C. Upstill-Goddard<sup>1</sup>

<sup>1</sup>Ocean Research Group, School of Marine Science and Technology, Newcastle University, Newcastle upon Tyne, UK

<sup>2</sup>Department of Applied Environmental Science, Stockholm University, Stockholm, Sweden

Received: 10 January 2014 – Accepted: 24 January 2014 – Published: 21 February 2014

Correspondence to: K. Schneider-Zapp (klaus.schneider-zapp@ncl.ac.uk)

Published by Copernicus Publications on behalf of the European Geosciences Union.

**An automated gas exchange tank for natural seawater samples**

K. Schneider-Zapp et al.

Title Page

Abstract

Introduction

Conclusions

References

Tables

Figures

⏪

⏩

◀

▶

Back

Close

Full Screen / Esc

Printer-friendly Version

Interactive Discussion

## Abstract

In order to advance understanding of the role of seawater surfactants in the air–sea exchange of climatically active trace gases via suppression of the gas transfer velocity ( $k_w$ ), we constructed a fully automated, closed air-water gas exchange tank and coupled analytical system. The system allows water-side turbulence in the tank to be precisely controlled with an electronically operated baffle. Two coupled gas chromatographs and an integral equilibrator, connected to the tank in a continuous gas-tight system, allow temporal changes in the partial pressures of SF<sub>6</sub>, CH<sub>4</sub> and N<sub>2</sub>O to be measured simultaneously in the tank water and headspace at multiple turbulence settings, during a typical experimental run of 3.25 h. PC software developed by the authors controls all operations and data acquisition, enabling the optimisation of experimental conditions with high reproducibility. The use of three gases allows three independent estimates of  $k_w$  for each turbulence setting; these values are subsequently normalised to a constant Schmidt number for direct comparison. The normalised  $k_w$  estimates show close agreement. Repeated experiments with MilliQ water demonstrate a typical measurement accuracy of 4% for  $k_w$ . Experiments with natural seawater show that the system clearly resolves the effects on  $k_w$  of spatial and temporal trends in natural surfactant activity. The system is an effective tool with which to probe the relationships between  $k_w$ , surfactant activity and biogeochemical indices of primary productivity, and should assist in providing valuable new insights into the air–sea gas exchange process.

## 1 Introduction

Air–sea gas exchange is a critical global process, providing the fundamental link between reactive trace gas production and consumption in the oceans and global atmospheric processes. For example, the oceans are the largest single sink for tropospheric carbon dioxide (CO<sub>2</sub>) (Khatiwala et al., 2009), contribute around one-third

OSD

11, 693–733, 2014

## An automated gas exchange tank for natural seawater samples

K. Schneider-Zapp et al.

Title Page

Abstract

Introduction

Conclusions

References

Tables

Figures

⏪

⏩

◀

▶

Back

Close

Full Screen / Esc

Printer-friendly Version

Interactive Discussion



## An automated gas exchange tank for natural seawater samples

K. Schneider-Zapp et al.

Title Page

Abstract

Introduction

Conclusions

References

Tables

Figures

◀

▶

◀

▶

Back

Close

Full Screen / Esc

Printer-friendly Version

Interactive Discussion



of tropospheric nitrous oxide ( $\text{N}_2\text{O}$ ) (IPCC, 2007) and make significant contributions to the global biogeochemical budgets of several other climate-active gases including methane ( $\text{CH}_4$ ), carbon monoxide ( $\text{CO}$ ), dimethyl sulphide ( $\text{CH}_3\text{SCH}_3$ ) and some other sulphur gases, and a range of halocarbons and hydrocarbons (Upstill-Goddard, 2011).

5 Understanding the physical and biogeochemical controls of air–sea gas exchange is therefore necessary for establishing biogeochemical models for predicting regional and global scale trace gas fluxes and feedbacks.

For a sparingly soluble gas, which applies to almost all gases of global biogeochemical interest, the flux  $F$  (e.g.  $\text{mol m}^{-2} \text{d}^{-1}$ ) across the air–sea interface can be considered as a diffusion-limited process in a typically  $20 \mu\text{m}$  to  $200 \mu\text{m}$  thick “diffusive sub-layer” on the water-side of the interface (Jähne, 2009). It can be written as the product of the driving force, i.e. its concentration difference between air  $C_a$  and sea water  $C_w$  (e.g.  $\text{mol m}^{-3}$ ), and the air–sea gas transfer velocity  $k_w$  (e.g.  $\text{cm h}^{-1}$ ):

$$15 \quad F = k_w(\alpha C_a - C_w), \quad (1)$$

where  $\alpha$  is the Ostwald solubility coefficient. Similar equations apply to the exchange of heat and momentum. The concentration difference term ( $\alpha C_a - C_w$ ) can be directly measured quite routinely but  $k_w$  cannot. Moreover, the magnitude of  $k_w$  varies with the degree of near-surface turbulence; increasing turbulence reduces the depth of the diffusive sub-layer, resulting in an increase in  $k_w$ . Indirect approaches are therefore required to estimate  $k_w$  in-situ and evaluate its variability in response to environmental forcing functions generating turbulence. One often used method for in-situ measurement is the so-called “dual tracer technique”, which measures the relative rates of evasion to air of two purposefully released, inert volatile tracers: sulphur hexafluoride ( $\text{SF}_6$ ) and helium-3 ( $^3\text{He}$ ). Temporal changes in the ratio of their seawater concentrations, typically measured over 24 h to 48 h time intervals, are used to derive  $k_w$  estimates which are then scaled to corresponding values for  $\text{CO}_2$  and other reactive trace gases of interest, using diffusivity based relationships (Wanninkhof et al., 1993; Wanninkhof et al., 1997; Watson et al., 1991; Nightingale et al., 2000). The dual tracer technique is however











output voltage is converted to a digital signal using a USB-6008 (12 bit) ADC (National Instruments, USA). Temperature in the tank water phase is recorded on an autonomous mini data logger (Minilog 8, Vemco, Canada; accuracy 0.2 °C) that is retrieved for data download at the end of each experiment.

### 3.2 Equilibration Vessel

The analysis of dissolved gases by gas chromatography necessitates either a pre-extraction or equilibration step, followed by the measurement of gas partial pressures in the resulting gas phase and corrections for air and water volumes and gas solubilities (Upstill-Goddard et al., 1996). Extraction techniques often involve pre-concentration procedures which can be complicated and the overall extraction efficiency can vary significantly. By contrast, automated gas equilibration has been shown to be highly reproducible (Upstill-Goddard et al., 1996). We therefore incorporated a water-air equilibration vessel as an integral component of the gas exchange tank apparatus. The equilibration vessel has a total internal volume of 183 cm<sup>3</sup> and has two principal components: a glass vessel equilibrator and a removable stainless steel equilibration manifold (Fig. 3). The design derives from a system we constructed for the high precision analysis of dissolved gases at sea (Upstill-Goddard et al., 1996). The equilibration manifold comprises three lengths of stainless steel tubing silver-soldered through a tapered stainless steel plug machined to seat precisely in the neck of the glass vessel to give a gas-tight seal. Two tubes are cut flush to the base of the plug and a third is connected to a stainless steel aerator frit near the bottom of the glass vessel. The frit is a standard chromatography solvent filter (Thames Restek, UK). The equilibration vessel has three water inlet/outlets (all 4 mm i.d.), each connected via a short length of flexible Tygon<sup>®</sup> tubing to a solenoid (Burkert 0124 2/2 way for aggressive media, Burkert, Germany; W1-W3 in Fig. 3). A digital temperature sensor (DS18B20+; resolution 0.1°; accuracy < 0.5°: Maxim, USA) is housed in a side arm. A second side arm in the equilibrator neck houses a pressure transducer identical to that used for monitoring tank headspace pressures (Sect. 3.1). A cylinder containing compressed air of known

## An automated gas exchange tank for natural seawater samples

K. Schneider-Zapp et al.

Title Page

Abstract

Introduction

Conclusions

References

Tables

Figures

◀

▶

◀

▶

Back

Close

Full Screen / Esc

Printer-friendly Version

Interactive Discussion





than for our experiments with an earlier gas exchange tank (Upstill-Goddard et al., 2003).

## Determining equilibration volumes

The relative volumes of water to headspace  $V_a/V_w$  involved in the equilibration step must be accurately known in order to facilitate corrections for solubility-driven phase partitioning (Upstill-Goddard et al., 1996).  $V_w$  can be determined gravimetrically by repeatedly generating headspace in the equilibrator. By contrast, system configuration precludes directly measuring  $V_a$ . To overcome this we directly estimated  $V_a/V_w$  by equilibration, similar to Upstill-Goddard et al. (1996). The gas exchange tank was filled with 93 L MilliQ water (resistivity typically  $18.2 \text{ M}\Omega \text{ cm}^{-3}$ ; Millipore Corporation, USA) enriched with  $\text{SF}_6$ ,  $\text{N}_2\text{O}$ , and  $\text{CH}_4$ , sealed and equilibrated by operating the baffle until the gas partial pressures in both the equilibrator headspace and in the tank headspace remained constant for  $> 12 \text{ h}$ . For this measurement ultra high purity (UHP)  $\text{N}_2$  ( $> 99.999\%$   $\text{N}_2$ , no detectable  $\text{SF}_6$ ,  $\text{N}_2\text{O}$  or  $\text{CH}_4$ ) was used as equilibrator gas, i. e.  $C_0 = 0$ . Concentrations in the tank headspace and equilibrator were then determined multiple times and averaged. These values were used together with the appropriate Ostwald solubilities of  $\text{SF}_6$  (Bullister et al., 2002),  $\text{CH}_4$  (Wiesenburg and Guinasso, 1979) and  $\text{N}_2\text{O}$  (Weiss and Price, 1980) at the temperature and pressure of equilibration and the tank headspace and water volumes, to calculate  $V_a/V_w$  according to Eq. (17). For the system as currently configured  $V_a/V_w = 0.79 \pm 0.02$ .

## 3.3 Wave height gauge

A capacitance-type high-precision wave height gauge (AWP-24; 30 cm double strand sensing wire, Akamina Technologies, Canada) is used. Analogue output voltage is digitised at 400 Hz (USB-6008 ADC, National Instruments, USA). The output voltage of the device is linearly proportional to the water level.

## An automated gas exchange tank for natural seawater samples

K. Schneider-Zapp et al.

Title Page

Abstract

Introduction

Conclusions

References

Tables

Figures

◀

▶

◀

▶

Back

Close

Full Screen / Esc

Printer-friendly Version

Interactive Discussion



## An automated gas exchange tank for natural seawater samples

K. Schneider-Zapp et al.

Title Page

Abstract

Introduction

Conclusions

References

Tables

Figures

◀

▶

◀

▶

Back

Close

Full Screen / Esc

Printer-friendly Version

Interactive Discussion



The probe is routinely calibrated to determine the relationship between water depth and output voltage by filling the gas exchange tank with sample water and progressively immersing the probe step-wise into the water. This is done by mounting the probe on a rod with precisely machined holes at 1 cm intervals. For each step the rod is bolted through one of the holes to a sturdy mount secured to the tank. After waiting for the water surface to settle, the output voltage is averaged over 10 s. A line is fitted to the immersion depth – voltage relation.

### 3.4 Ancillary measurements

Absolute pressure ( $P_0$ ) and temperature ( $T$ ) in the laboratory are measured using a digital sensor (Sensortec BMP085; pressure range 300–1100 hPa; absolute pressure accuracy 1 hPa; absolute temperature accuracy 0.5°: Bosch, Germany).

### 3.5 Gas chromatography

The need to determine the partial pressures of SF<sub>6</sub>, CH<sub>4</sub> and N<sub>2</sub>O in both the air and water phases during an experiment precludes using a single GC; this would necessitate long sampling intervals and/or a long experimental duration, with consequent loss of experimental resolution. Therefore two identically configured GC's were used (both HP 5890), one for analysing tank headspace (“air-phase GC”) and one for analysing equilibrator air following water sample equilibration (“water phase GC”). The analysis is identical in each GC, being isothermal (60°) and based on methods developed in our laboratory (Upstill-Goddard et al., 1990, 1996, 2003). A schematic is shown in Fig. 4. A series of motor-driven stainless steel chromatography valves, V1–V5 in Fig. 4 (Valco: Vici AG, Switzerland), allow the selective switching of tank headspace, equilibrator headspace and calibration standards onto the separating columns (one each for SF<sub>6</sub>, N<sub>2</sub>O and CH<sub>4</sub> in each GC) and detectors, via fixed volume sample loops (internal volume: SF<sub>6</sub> 10 mL, CH<sub>4</sub> 1 mL, N<sub>2</sub>O 1.5 mL). Chromatographic separation of SF<sub>6</sub> is on Molecular Sieve 5A columns (4m × 1.75 mm i. d.), whereas N<sub>2</sub>O and CH<sub>4</sub> are

## An automated gas exchange tank for natural seawater samples

K. Schneider-Zapp et al.

Title Page

Abstract

Introduction

Conclusions

References

Tables

Figures

⏪

⏩

◀

▶

Back

Close

Full Screen / Esc

Printer-friendly Version

Interactive Discussion



both separated on 80–100 mesh Porapak Q columns ( $\text{CH}_4$ ,  $4\text{ m} \times 1.75\text{ mm i. d.}$ ;  $\text{N}_2\text{O}$ ,  $5\text{ m} \times 1.75\text{ mm i. d.}$ ). The GC carrier gas is UHP  $\text{N}_2$ . Flow rates are typically around  $25\text{ cm}^3\text{ min}^{-1}$  for  $\text{CH}_4$  and  $\text{N}_2\text{O}$ , and  $50\text{ cm}^3\text{ min}^{-1}$  for  $\text{SF}_6$ . Water vapour produced during sample equilibration is removed using  $\text{Mg}(\text{ClO}_4)_2$  and  $\text{CO}_2$  is removed using  $\text{NaOH}$  (Upstill-Goddard et al., 1996). Detection of  $\text{CH}_4$  uses a flame ionization detector (FID) at  $300^\circ$  whereas detection of  $\text{N}_2\text{O}$  and  $\text{SF}_6$  uses an Electron Capture Detector (ECD) with a  $^{63}\text{Ni}$  source at  $350^\circ$ .

The GC responses are integrated automatically using proprietary GC software (Clarity: DataApex, Prague, Czech Republic). Method calibration uses a series of mixed calibration standards prepared by pressure dilution in UHP  $\text{N}_2$  (Upstill-Goddard et al., 1990, 1996). Analytical precisions are typically  $\pm 1\%$   $\text{CH}_4$ ,  $\pm 0.8\%$   $\text{N}_2\text{O}$ , and  $\pm 1\%$   $\text{SF}_6$ . All three gases are analysed in less than 8 min.

### 3.6 Limits of detection

Minimum detectable levels of  $\text{SF}_6$ ,  $\text{N}_2\text{O}$  and  $\text{CH}_4$  have been determined by estimating the detector responses corresponding to a signal to baseline noise ratio of 2 and dividing by the detector peak width (peak area/peak height) in seconds (Upstill-Goddard et al., 1996). Minimum detectable levels are 0.5 pptv  $\text{SF}_6$ , 0.2 ppbv  $\text{N}_2\text{O}$  and 10 ppbv  $\text{CH}_4$ . However, in practice the partial pressures of all three gases in the equilibrator gas combined with solubility considerations (Bullister et al., 2002; Wiesenburg and Guinasso, 1979; Weiss and Price, 1980) preclude operating the detectors close to these limits.

## 4 Experimental procedure

Prior to use all ancillary equipment is thoroughly cleaned with ethanol and rinsed with MilliQ water. All metal and glassware is subsequently baked at  $450^\circ$  overnight.





This effect cannot be separated from the statistical error or corrected for, as the drift is irregular.

Estimates of  $k_w$  are obtained from Eq. (13) using weighted linear regression (Sect. 4.4.1). The uncertainty is estimated from the weighted fit. The  $k_w$  estimates are then scaled to Schmidt number 660 using Eq. (19) (Sect. 4.4.3). Convention is to scale all measured values of  $k_w$  to Schmidt numbers of either 660 or 600, being the values for CO<sub>2</sub> in freshwater and salinity 35 seawater respectively, at 20 °C. Schmidt numbers are obtained from Wanninkhof (1992). From the MilliQ data, a Schmidt number exponent of  $n = 1/2$  was determined using Eq. (20), corresponding to a flat surface. This is reasonable, because the baffle generated turbulence does not create much surface turbulence (e.g. capillary waves) compared to wind drag (see also the introduction, Sect. 1).

The wave frequency energy spectrum is calculated from the sampled wave height using the method of Welch (1967) (see Harris, 1978, for more information) with a Hann window of length 131 072.

### 4.3 Surfactant measurement

Surfactant activity (SA) is measured using AC voltammetry (Ćosović and Vojvodić, 1982) (Metrohm 797 VA Computrace, Metrohm, Switzerland) with a hanging mercury drop, a silver/silver chloride reference electrode and a platinum wire auxiliary electrode. Samples are brought to salinity 35 prior to measurement by adding surfactant-free NaCl solution. For each measurement, a new mercury drop is created and the first few drops discarded. Surfactants accumulate on the drop at  $V = -0.6V$  for 15 s or 60 s with stirring (1000 rpm). Alternating voltage scans of 10 mV at 75 Hz produce a current which is measured. Instrument calibration uses the non-ionic soluble surfactant Triton T-X-100. Each response is corrected for the added NaCl solution and expressed as an equivalent T-X-100 concentration.

## An automated gas exchange tank for natural seawater samples

K. Schneider-Zapp et al.

Title Page

Abstract

Introduction

Conclusions

References

Tables

Figures

⏪

⏩

◀

▶

Back

Close

Full Screen / Esc

Printer-friendly Version

Interactive Discussion



## 4.4 Theory

### 4.4.1 Tank gas exchange

For a sealed gas exchange tank containing seawater and air and without gas sources or sinks, Eq. (1) can be used to derive a mass balance:

$$5 \quad \left( \frac{\partial C_a}{\partial t} V_a \right) = k_w \left( C_w - \alpha C_a \right) A. \quad (2)$$

10 The solubility  $\alpha$ , volumes  $V_a$  and  $V_w$ , and surface area  $A$  are assumed to be constant. In reality,  $\alpha$  depends on temperature. In practice changes in experimental temperature are of the order of  $0.5^\circ$ . For such a change in temperature at  $20^\circ$ , the change in  $\alpha$  is  $< 1.6\%$  for  $\text{SF}_6$ ,  $< 1.4\%$  for  $\text{N}_2\text{O}$  and  $< 1\%$  for  $\text{CH}_4$  according to published parameterisations (Bullister et al., 2002; Wiesenburg and Guinasso, 1979; Weiss and Price, 1980).

Let the height of phase  $i$  (i. e. air a or water w) be  $h_i$ , i.e.  $h_i := V_i/A$ , and let

$$D := C_w - \alpha C_a. \quad (3)$$

15 For  $\text{SF}_6$ , which has a very low solubility (Bullister et al., 2002),  $D \approx C_w$  for all practical purposes. In contrast, for  $\text{CH}_4$  and  $\text{N}_2\text{O}$ , which are one and two orders of magnitude more soluble respectively than  $\text{SF}_6$  (Wiesenburg and Guinasso, 1979; Weiss and Price, 1980) the value of  $C_a$  must be taken account of. Re-arranging Eq. (3), taking the derivative and using the chain rule results in

$$20 \quad \frac{\partial C_a}{\partial t} = \frac{1}{\alpha} \left[ \frac{\partial C_w}{\partial t} - \frac{\partial D}{\partial t} \right] = \frac{k_w}{h_a} D, \quad (4)$$

## An automated gas exchange tank for natural seawater samples

K. Schneider-Zapp et al.

Title Page

Abstract

Introduction

Conclusions

References

Tables

Figures

⏪

⏩

◀

▶

Back

Close

Full Screen / Esc

Printer-friendly Version

Interactive Discussion



where Eq. (2) (top) has been used in the last equality. Substituting  $\frac{\partial C_w}{\partial t}$  into Eq. (2) (bottom), a differential equation in  $D$  is obtained:

$$\frac{\partial D}{\partial t} + k_w \underbrace{\left[ \frac{1}{h_w} + \frac{\alpha}{h_a} \right]}_{=: \beta} = 0 \quad (5)$$

5 Solving this gives

$$D = D_0 \exp(-k_w \beta t), \quad (6)$$

where  $D_0 := D(t = 0)$ .

10 Due to conservation of mass, the total amount of gas  $N$  in the system must remain constant. Hence:

$$N = C_a V_a + C_w V_w = \text{const.} \quad (7)$$

15 This relation serves as a routine check of the experimental results and system integrity; a change in the value of  $N$  during the experiment implies system leaks and/or defective chromatography.

At each equilibration step the tank water volume  $V_w$  decreases (here assumed instantaneously) by volume  $V_s$ , such that  $V_{w>} = V_{w<} - V_s$ , where  $V_{w<}$  and  $V_{w>}$  are the tank water volumes before and after drawing the sample, respectively. The effect is to change the value of  $\beta$  so that the differential equation no longer has constant coefficients. However, within each interval  $[t_n, t_{n+1}]$  between two measurements at times  $t_n$  and  $t_{n+1}$ , the volumes are constant and Eq. (6) can be used. At each sampling step the values of the coefficients change instantaneously; the variables at the end of the previous interval become the initial conditions for the next interval. If  $V_{e,n} = nV_s$  is the total water volume already extracted at  $t_n$ , using the abbreviations  $V_{w,n} := V_w|_{t=t_n}$ ,  $D_n := D(t = t_n)$  and

$$25 \beta_n := \beta|_{t=t_n} = \frac{A}{V_{w,n-1} - V_s} + \frac{A\alpha}{V_a} = \frac{A}{V_{w,0} - nV_s} + \frac{A\alpha}{V_a} = \frac{1}{h_{w,0} - nh_s} + \frac{\alpha}{h_a} \quad (8)$$

**An automated gas exchange tank for natural seawater samples**

K. Schneider-Zapp et al.

Title Page	
Abstract	Introduction
Conclusions	References
Tables	Figures
◀	▶
◀	▶
Back	Close
Full Screen / Esc	
Printer-friendly Version	
Interactive Discussion	



derives

$$D_n = D_{n-1} \exp(-k_w \beta_n (t_n - t_{n-1})) \quad (9)$$

The first water sample is drawn at  $t_0$ , the experiment starts running with the reduced water volume  $V_w - V_s$  and thus the system response is

$$D_n = D_0 \exp \left( -k_w \sum_{j=1}^n \beta_j (t_j - t_{j-1}) \right) \quad (10)$$

Note that for  $n = 0$ , the sum is zero and the equation is identical to the original Eq. (6). The new solution Eq. (10) is not in the form  $\exp -k_w \beta t$  but has a sum of different  $t_j$  in its exponential. It can be solved for  $k_w$ ; however it diverges for  $n = 0$ . This is overcome by conversion to the form  $\exp -k_w \beta t$  as

$$D_n = D_0 \exp \left( -k_w \underbrace{\left[ \sum_{j=1}^n \beta_j \frac{t_j - t_{j-1}}{t_n - t_0} \right]}_{=: B_n} (t_n - t_0) \right) \quad (11)$$

with

$$B_n := \sum_{j=1}^n \beta_j \frac{t_j - t_{j-1}}{t_n - t_0} = \frac{A}{t_n - t_0} \sum_{j=1}^n \frac{t_j - t_{j-1}}{V_{w,0} - jV_s} + \frac{A\alpha}{V_a} \quad (12)$$

Note that  $B_0 = \beta_0$  (eqs. 11 and 6). For  $V_s = 0$ , we obtain  $B_n = \beta_0$  and the solution reduces to Eq. (6) with  $t_0 = 0$ . With  $V_s > 0$ , the value of  $B_n$  increases (the denominator in each summand is decreased) and consequently  $D$  decreases progressively more rapidly with increasing experimental run time during which further water is extracted

from the tank. Consequently some fraction of the decrease in  $D$  is due to volume extraction. Without any correction for this  $k_w$  is overestimated. The factor  $\frac{t_j - t_{j-1}}{t_n - t_0}$  is applied as a weight factor for any given water volume during the experiment.

The solution can be expressed in logarithmic form to derive a linear fit obtaining  $k_w$  as

$$\chi_n := \frac{1}{B_n} \ln \frac{D_0}{D_n} = k_w(t_n - t_0). \quad (13)$$

The mass balance Eq. (7) also has to be adjusted to account for the water loss on sampling:

$$N_n = V_{w,n} C_{w,n} + \sum_{j=1}^n C_{w,j-1} V_s + V_a C_{a,n}. \quad (14)$$

#### 4.4.2 Water sample equilibration

We can consider a water sample of volume  $V_w$  in the equilibrator with an initial dissolved gas concentration  $C_w$  at in situ pressure  $P_1$  and temperature  $T_1$ . The number of moles of gas in the water is  $N_1 = C_w V_w$ .

The water sub-sample then equilibrates with a head space of volume  $V_a$  and initial gas concentration  $C_0$ . The total number of moles of gas in the equilibrator is then  $N = N_1 + N_0 = V_w C_w + V_a C_0$ . During equilibration the gas partitions according to  $\alpha C'_a = C'_w$ , where  $\alpha$  is the Ostwald solubility coefficient.  $N$  remains constant (conservation of mass), thus

$$V_a C'_a + V_w C'_w = V_a C'_a + V_w \alpha C'_a = V_a C_0 + V_w C_w. \quad (15)$$

Solving for  $C_w$  results in

$$C_w = \frac{V_a}{V_w} (C'_a - C_0) + \alpha C'_a, \quad (16)$$

## An automated gas exchange tank for natural seawater samples

K. Schneider-Zapp et al.

Title Page

Abstract

Introduction

Conclusions

References

Tables

Figures

◀

▶

◀

▶

Back

Close

Full Screen / Esc

Printer-friendly Version

Interactive Discussion



which can be used to back-calculate the gas concentration in the water sample using  $C'_a$ .

For evaluating Eq. (16), the water-headspace volume ratio  $V_a/V_w$  is required. It is determined by a measurement with known  $C_w$  and  $C'_a$  so that Eq. (15) is then solved for  $V_a/V_w$ :

$$\frac{V_a}{V_w} = \frac{C_w - \alpha C'_a}{C'_a - C_0} \quad (17)$$

#### 4.4.3 Schmidt number scaling

The value of  $k_w$  for any gas is a function of its Schmidt number  $Sc$ , which is defined as the ratio of the viscosity of water to the corresponding gas diffusivity at the requisite temperature, i.e.  $Sc = \nu/D$ . Theory predicts the scaling

$$k_w = \frac{u_*}{R} Sc^{-n} \quad (18)$$

where  $u_*$  is the friction velocity,  $R$  is the resistance for momentum transfer and the exponent  $n$  is equal to  $2/3$  for a smooth surface and  $1/2$  for a rough surface with a smooth transition (Richter and Jähne, 2010). This relation allows the interconversion of  $k_w$  for any given gas to  $k_w$  for any other specified gas. Given two gases 1 and 2 with transfer velocities  $k_{w1}$  and  $k_{w2}$  and Schmidt numbers  $Sc_1$  and  $Sc_2$ , respectively, one obtains

$$k_{w1} = \left( \frac{Sc_1}{Sc_2} \right)^{-n} k_{w2} \quad (19)$$

Simultaneous measurements of two gases with different Schmidt numbers can be used to calculate the exponent:

$$n = \frac{\ln \frac{k_{w1}}{k_{w2}}}{\ln \frac{Sc_2}{Sc_1}} = \frac{\ln \frac{k_{w1}}{k_{w2}}}{\ln \frac{D_1}{D_2}} \quad (20)$$

**An automated gas exchange tank for natural seawater samples**

K. Schneider-Zapp et al.

Title Page	
Abstract	Introduction
Conclusions	References
Tables	Figures
◀	▶
◀	▶
Back	Close
Full Screen / Esc	
Printer-friendly Version	
Interactive Discussion	



#### 4.4.4 Wave spectra

Let  $\eta(\mathbf{x}, t)$  be the (vertical) surface displacement from the mean surface level at horizontal position  $\mathbf{x} = (x_1, x_2)$  and time  $t$ . Its mean value is zero, i.e.  $\langle \eta \rangle = 0$ . The higher moments of the displacement are important for characterising the wave field.

5 The autocorrelation function of  $\eta$  is

$$\begin{aligned}
 R(\xi, \tau) &= \langle \eta(\mathbf{x}, t) \eta(\mathbf{x} + \xi, t + \tau) \rangle \\
 &= \lim_{\mathbf{x} \rightarrow \infty} \lim_{T \rightarrow \infty} \frac{1}{X_1 X_2 T} \int_0^{\mathbf{x} T} \int_0^T \eta(\mathbf{x}, t) \eta(\mathbf{x} + \xi, t + \tau) d\mathbf{x} dt \\
 &= \lim_{\mathbf{x} \rightarrow \infty} \lim_{T \rightarrow \infty} \frac{1}{X_1 X_2 T} (\eta(\mathbf{x}, t) * \eta(-\mathbf{x}, -t))(\xi, \tau),
 \end{aligned} \tag{21}$$

where the  $*$  operator indicates convolution,

$$(a * b)(\tau) = \int_{-\infty}^{\infty} a(t) b(\tau - t) dt. \tag{22}$$

10

The autocorrelation function is the same as the autocovariance, since  $\langle \eta \rangle = 0$ , thus it indicates how the displacement at different locations and times is correlated.

The wave energy density spectrum is defined as the Fourier transform of the autocorrelation (Phillips, 1980)

$$15 \quad X(\mathbf{k}, \omega) = \hat{R}(\mathbf{k}, \omega) := \frac{1}{(2\pi)^3} \int_{\mathbb{R}^2} \int_{\mathbb{R}} R(\xi, \tau) e^{-i(\mathbf{k}\xi - \omega\tau)} d\xi d\tau \tag{23}$$

with wave number  $\mathbf{k}$  and angular frequency  $\omega$ .

Since a waveprobe can only measure the temporal change of the surface displacement  $\eta(t) := \eta(0, t)$ , the measurement will only be able produce an estimate of the

frequency energy spectrum

$$\Phi(\omega) := \int_{\mathbb{R}^2} X(\mathbf{k}, \omega) d\mathbf{k} = \lim_{T \rightarrow \infty} \frac{2\pi}{T} |\hat{\eta}(\omega)|^2. \quad (24)$$

Parseval's theorem states that the integral over space and time is equal to the integral in Fourier space,

$$\int_{\mathbb{R}^2} \int_{\mathbb{R}} |\eta(\mathbf{x}, t)|^2 dx dt = (2\pi)^3 \int_{\mathbb{R}^2} \int_{\mathbb{R}} |\hat{\eta}(\mathbf{k}, \omega)|^2 d\mathbf{k} d\omega, \quad (25)$$

which describes energy conservation. This enables a check as to whether the normalisation has been satisfactorily carried out.

## 5 Results and discussion

### 5.1 Evaluation procedure

To test the evaluation procedure synthetic data were used. After choosing a nominal value of  $k_w$ , an initial condition  $C_{w,0}$ ,  $C_{a,0}$ , and constants  $T$  and  $S$ , the true system response was calculated using Eq. (10), with volumes and dimensions from the experimental setup. Gaussian noise with mean 0 and variance of 2% was added to the true gas concentrations to model the measurement process. The data were then put into the evaluation procedure. The original transfer velocity  $k_w$  was always within the uncertainty of the estimated transfer velocity.

### 5.2 MilliQ experiments

A number of experiments with MilliQ water were conducted to validate the experiment and to test the reproducibility. Figure 7 shows the mass balance, i.e. the total amount of

## An automated gas exchange tank for natural seawater samples

K. Schneider-Zapp et al.

Title Page

Abstract

Introduction

Conclusions

References

Tables

Figures

⏪

⏩

◀

▶

Back

Close

Full Screen / Esc

Printer-friendly Version

Interactive Discussion



gas within the tank, for a typical exchange experiment. Deviations are within the error, proving that the setup is gas-tight, i.e. no gas is lost or acquired during the run.

Estimated values of  $k_{660}$  ( $k_w$  scaled to a Schmidt number of 660) derived from  $\text{CH}_4$  and  $\text{SF}_6$  for 6 different MilliQ experiments are shown in Fig. 8. Weighted means and standard deviations of these data are summarised in Table 1. For individual experiments the two independent  $k_{660}$  estimates show very close agreement; any small discrepancies most likely include uncertainties in the Schmidt number values and the solubility parameterisations. Thus, even in the worst case changes of  $2 \text{ cm h}^{-1}$  are significant with 95 % probability; for the baffle speed of  $0.6 \text{ Hz}$  the significance level is  $1.2 \text{ cm h}^{-1}$  with 95 % probability. The weighted standard deviation is 4 % for all baffle speeds and both gases.

Wave spectra for a selected experiment are shown in Fig. 9. As expected, the wave energy is higher for higher baffle frequencies. The first peak for each boundary condition corresponds to the respective baffle speed, showing that the baffle has a reproducible and stable frequency. Further peaks at higher frequencies are the harmonics caused by reflection and refraction inside the tank.

### 5.3 Seawater experiments

Estimated values of  $k_w$  from the coastal North Sea transects, derived from  $\text{CH}_4$  at a baffle speed of  $0.6 \text{ Hz}$ , are shown in Fig. 10 (top). For the winter transect (13 February 2013)  $k_w$  was between  $(12.4 \pm 0.3) \text{ cm h}^{-1}$  (near-shore) and  $(13.2 \pm 0.2) \text{ cm h}^{-1}$  (off-shore), while corresponding autumn (4 October 2012) values were between  $(9.4 \pm 0.3) \text{ cm h}^{-1}$  (near-shore) and  $(11.6 \pm 0.2) \text{ cm h}^{-1}$  (off-shore). Comparison with Fig. 10 (bottom), which shows surfactant activity (SA) in the SML samples, clearly shows these spatial and temporal differences in  $k_w$  to be a function of SA. The spatial gradients in  $k_w$  are consistent with a decreasing influence of terrestrially derived surfactants in river outflow with distance offshore. Higher  $k_w$  suppression by surfactant during the autumn reflects higher SA arising from primary productivity, whereas lower

## An automated gas exchange tank for natural seawater samples

K. Schneider-Zapp et al.

Title Page

Abstract

Introduction

Conclusions

References

Tables

Figures

◀

▶

◀

▶

Back

Close

Full Screen / Esc

Printer-friendly Version

Interactive Discussion

winter suppression presumably reflects lower SA arising from surfactant degradation processes.

For the most landwards station of the autumn transect (low  $k_w$ ) and the most offshore station from the winter transect (high  $k_w$ ),  $k_w$  vs. baffle frequency is shown for CH<sub>4</sub> and SF<sub>6</sub> in Fig. 11. The agreement between the two gases is acceptable, the discrepancies being largely attributable to uncertainties in the Schmidt number parameterisations, with additional small contributions arising from GC detector drift, which is somewhat larger for SF<sub>6</sub> than for CH<sub>4</sub>. Nevertheless, the observed trends are clearly significant within the analytical error. Our experimental procedures are evidently well suited to examine the relative natural variability of  $k_w$  between seawater samples containing varying levels of surfactant.

## 6 Conclusions

We have developed a laboratory gas exchange tank and associated analytical methodology that enables fully automated, routine determination of the gas transfer velocities of SF<sub>6</sub>, CH<sub>4</sub> and N<sub>2</sub>O in natural seawaters under strictly controlled conditions of turbulence. Repeated experiments with MilliQ water demonstrated a typical measurement accuracy of 4% for  $k_w$ . Experiments with natural seawater samples collected on two North Sea coastal transects showed a clear influence of surfactant activity on the strong spatial and temporal gradients in  $k_w$  that we observed. During ongoing and planned work, both in the coastal North Sea and in the open ocean, we aim to establish clear relationships between  $k_w$ , surfactant activity and biogeochemical indices of primary productivity. In so doing we hope to better understand the spatio-temporal variability of  $k_w$  and thereby, to contribute valuable new insights into the air–sea gas exchange process.

*Acknowledgements.* We wish to thank our colleagues in the workshop of the School of Marine Science and Technology at Newcastle for modifications to the basic tank structure and for installing the electronic components, and in the glassblowing workshop in the School of Chem-

### An automated gas exchange tank for natural seawater samples

K. Schneider-Zapp et al.

Title Page

Abstract

Introduction

Conclusions

References

Tables

Figures

⏪

⏩

◀

▶

Back

Close

Full Screen / Esc

Printer-friendly Version

Interactive Discussion





## An automated gas exchange tank for natural seawater samples

K. Schneider-Zapp et al.

Title Page

Abstract

Introduction

Conclusions

References

Tables

Figures

◀

▶

◀

▶

Back

Close

Full Screen / Esc

Printer-friendly Version

Interactive Discussion



- Gašparović, B.: Decreased production of surface-active organic substances as a consequence of the oligotrophication in the northern Adriatic Sea, *Estuar. Coast. Shelf Sc.*, 115, 33–39, doi:10.1016/j.ecss.2012.02.004, 2012. 696
- Goldman, J. C., Dennett, M. R., and Frew, N. M.: Surfactant effects on air–sea gas exchange under turbulent conditions, *Deep-Sea Res.*, 35, 1953–1970, doi:10.1016/0198-0149(88)90119-7, 1988. 696
- Harnisch, J. and Eisenhauer, A.: Natural CF<sub>4</sub> and SF<sub>6</sub> on Earth, *Geophys. Res. Lett.*, 25, 2401–2404, doi:10.1029/98GL01779, 1998. 698
- Harris, F. J.: On the use of windows for harmonic analysis with the discrete Fourier Transform, in: *Proceedings of the IEEE*, Vol. 66-1, 1978. 708
- IPCC: *Climate Change 2007 – The Physical Science Basis: Working Group I Contribution to the Fourth Assessment Report of the IPCC*, Cambridge University Press, Cambridge, UK and New York, NY, USA, 2007. 695, 698
- Jähne, B.: Air–sea gas exchange, in: *Encyclopedia Ocean Sciences*, edited by: Steele, J. H., Turekian, K. K., and Thorpe, S. A., 3434–3444, Elsevier, doi:10.1016/B978-0123744473-9.00642-1, 2009. 695
- Khalil, M.: *Atmospheric Methane: Sources, Sinks and Role in Global Change*, Springer, New York, 1993. 699
- Khatiwala, S., Primeau, F., and Hall, T.: Reconstruction of the history of anthropogenic CO<sub>2</sub> concentrations in the ocean, *Nature*, 462, 346–349, doi:10.1038/nature08526, 2009. 694
- McKenna, S. P. and McGillis, W. R.: The role of free-surface turbulence and surfactants in air–water gas transfer, *Int. J. Heat Mass Tran.*, 47, 539–553, 2004. 696
- Nevison, C. D. and Holland, E.: A reexamination of the impact of anthropogenically fixed nitrogen on Atmospheric N<sub>2</sub>O and the stratospheric O<sub>3</sub> layer, *J. Geophys. Res.*, 102, 25519–25536, doi:10.1029/97JD02391, 1997. 698
- Nightingale, P., Malin, G., Law, C. S., Watson, A. J., Liss, P. S., Liddicoat, M. I., Boutin, J., and Upstill-Goddard, R. C.: In situ evaluation of air–sea gas exchange parameterizations using novel conservative and volatile tracers, *Glob. Biogeochem. Sci.*, 14, 373–387, doi:10.1029/1999GB900091, 2000. 695, 698
- Phillips, O. M.: *The Dynamics of the Upper Ocean*, Cambridge University Press, New York, 1980. 714
- Prinn, R., Cunnold, D., Rasmussen, R., Simmonds, P., Alyea, F., Crawford, A., Fraser, P., and Rosen, R.: Atmospheric emissions and trends of nitrous oxide de-







## An automated gas exchange tank for natural seawater samples

K. Schneider-Zapp et al.

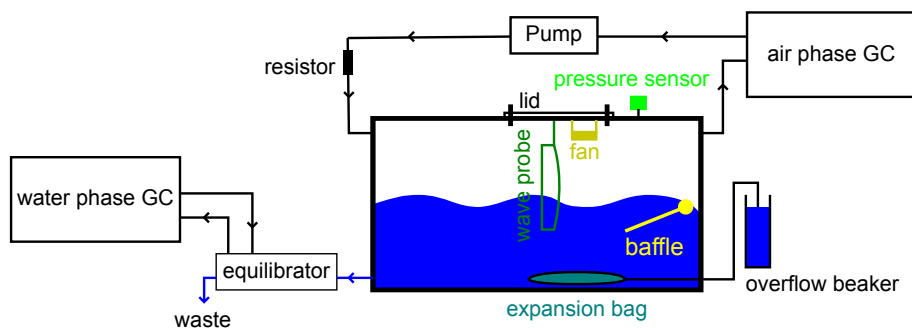


**Fig. 1.** Schematic of the gas exchange experiment. The seawater sample (93 L) is contained in a gas-tight tank ( $0.73\text{ m} \times 0.48\text{ m} \times 0.48\text{ m}$  internally). Water-side turbulence is created with a baffle driven by a stepper motor. An automatic equilibration circuit (details see Fig. 3) regularly takes water samples and equilibrates the water with an “equilibrator gas” of known  $\text{SF}_6$ ,  $\text{CH}_4$  and  $\text{N}_2\text{O}$  composition, before measuring resulting gas partial pressures in a gas chromatograph (GC). Air phase gas partial pressures are constantly measured with a second GC. Wave spectra at a single point are acquired with a capacitance wave probe. Pressure and temperature in the tank and the equilibrator as well as total ambient pressure are continuously monitored.

Title Page

Abstract

Introduction

Conclusions

References

Tables

Figures

◀

▶

◀

▶

Back

Close

Full Screen / Esc

Printer-friendly Version

Interactive Discussion

## An automated gas exchange tank for natural seawater samples

K. Schneider-Zapp et al.

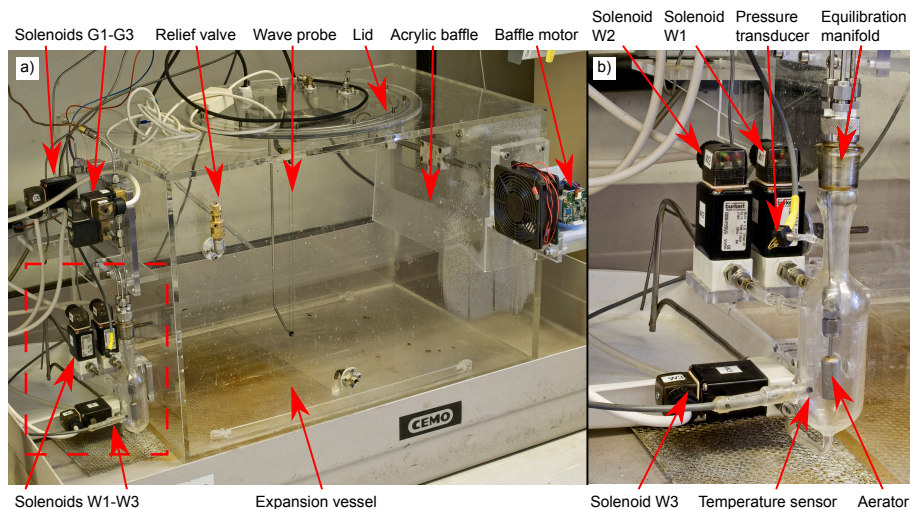


**Fig. 2.** Annotated photograph of the gas exchange apparatus: **(a)** the gas exchange tank. Note that the overflow vessel usually connected to the expansion vessel is omitted for clarity; **(b)** the equilibration vessel shown by the dashed red box in image **(a)**.

Title Page

Abstract

Introduction

Conclusions

References

Tables

Figures

◀

▶

◀

▶

Back

Close

Full Screen / Esc

Printer-friendly Version

Interactive Discussion

## An automated gas exchange tank for natural seawater samples

K. Schneider-Zapp et al.

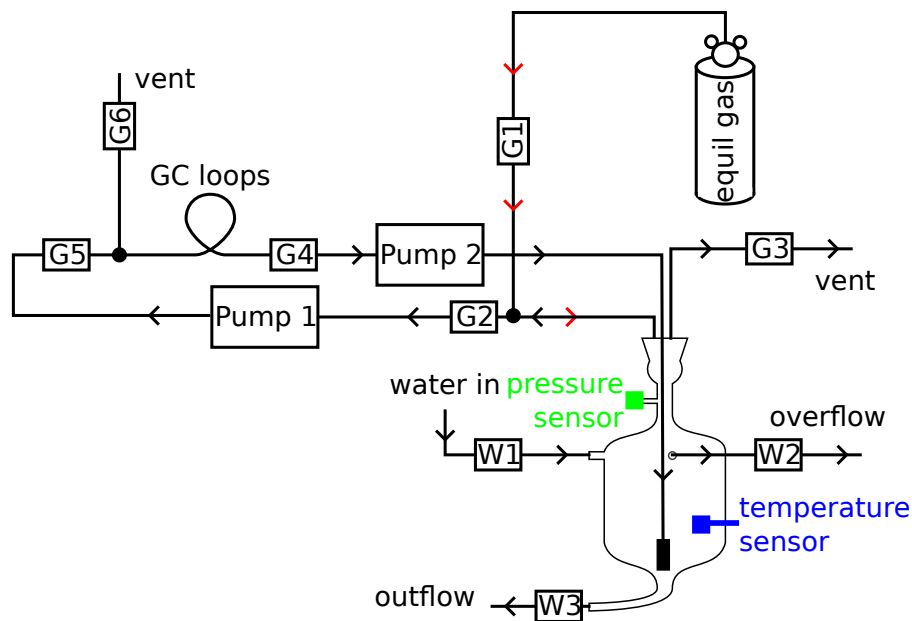


**Fig. 3.** Schematic of the equilibration system. For circuit operation see text.

Title Page

Abstract

Introduction

Conclusions

References

Tables

Figures

◀

▶

◀

▶

Back

Close

Full Screen / Esc

Printer-friendly Version

Interactive Discussion

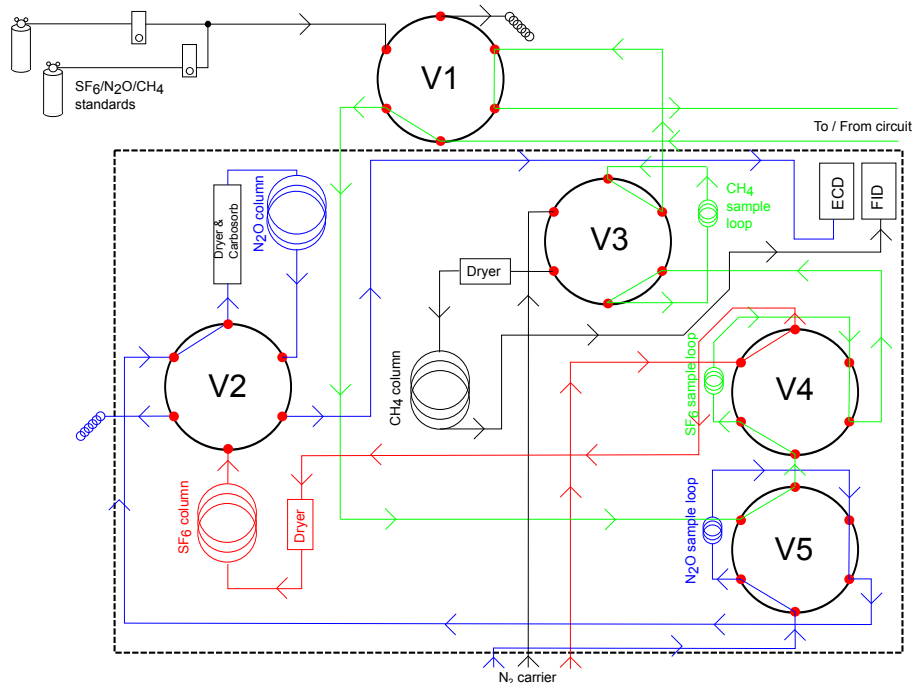


**Fig. 4.** Schematic of the GC system used to measure SF<sub>6</sub>, N<sub>2</sub>O, and CH<sub>4</sub>, here in N<sub>2</sub>O inject mode. Each sample loop can be injected separately using the corresponding valve (V3, V4, and V5, respectively). For the ECD, the N<sub>2</sub>O and the SF<sub>6</sub> column can be selected with valve V2. For detailed description see text.

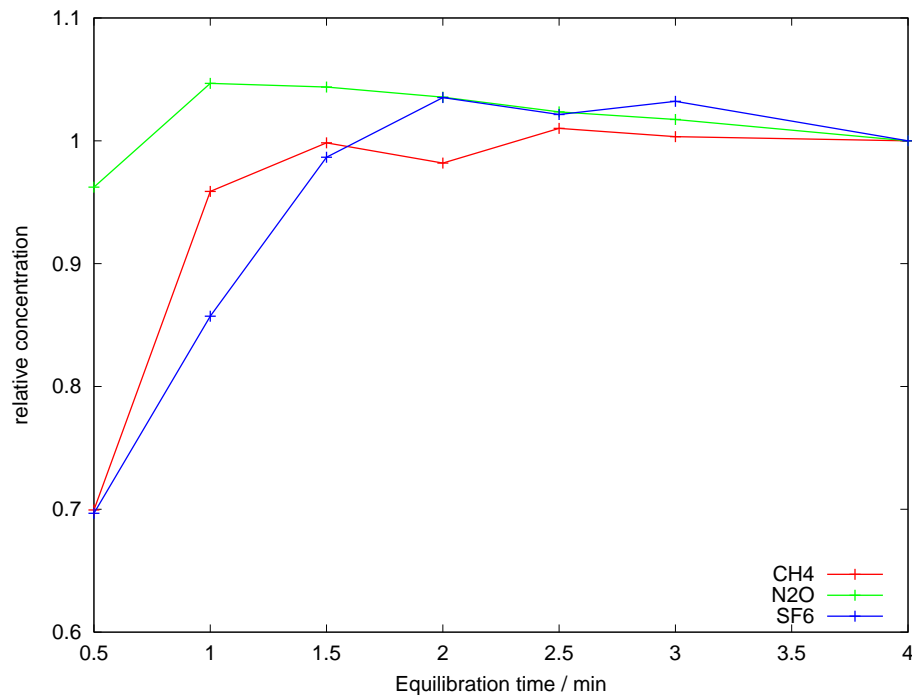
**An automated gas exchange tank for natural seawater samples**

K. Schneider-Zapp et al.

Title Page	
Abstract	Introduction
Conclusions	References
Tables	Figures
◀	▶
◀	▶
Back	Close
Full Screen / Esc	
Printer-friendly Version	
Interactive Discussion	

**An automated gas exchange tank for natural seawater samples**

K. Schneider-Zapp et al.

**Fig. 5.** Relative gas concentration vs. equilibration time for SF<sub>6</sub>, N<sub>2</sub>O, and CH<sub>4</sub>.[Title Page](#)[Abstract](#)[Introduction](#)[Conclusions](#)[References](#)[Tables](#)[Figures](#)[◀](#)[▶](#)[◀](#)[▶](#)[Back](#)[Close](#)[Full Screen / Esc](#)[Printer-friendly Version](#)[Interactive Discussion](#)

## An automated gas exchange tank for natural seawater samples

K. Schneider-Zapp et al.

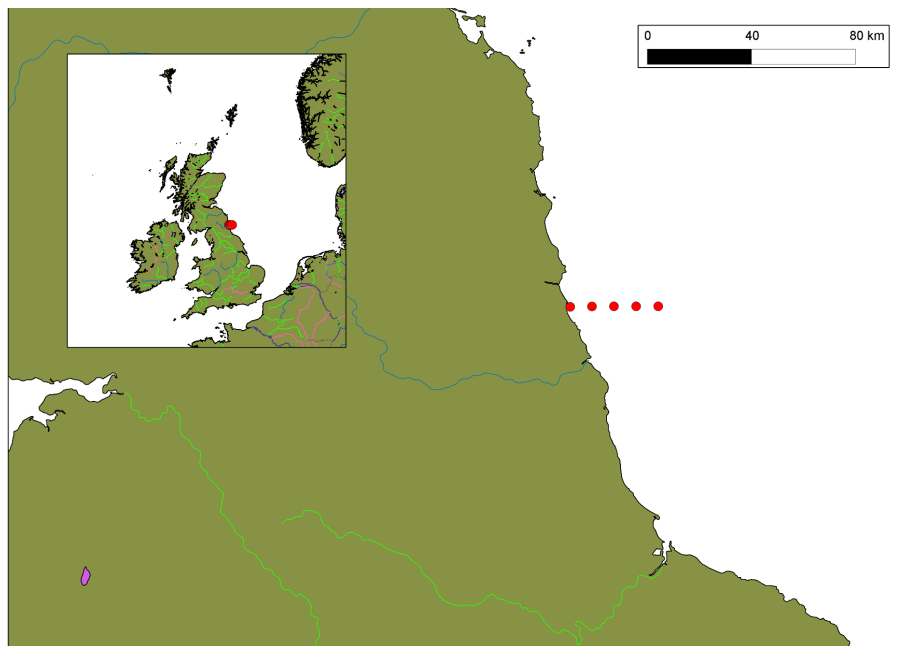


**Fig. 6.** The sampling stations (red circles) on the transects in the coastal North Sea off north-east England.

Title Page

Abstract

Introduction

Conclusions

References

Tables

Figures

◀

▶

◀

▶

Back

Close

Full Screen / Esc

Printer-friendly Version

Interactive Discussion



**An automated gas exchange tank for natural seawater samples**

K. Schneider-Zapp et al.

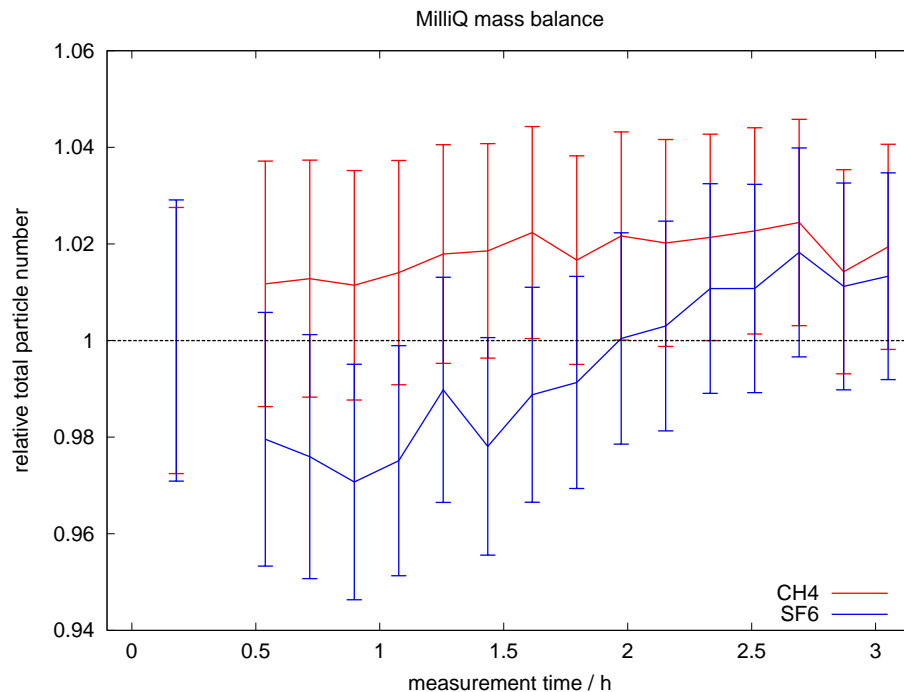


**Fig. 7.** Total amount of gas in the tank according to Eq. (14), normalised to the first measurement, vs. time of a typical gas exchange experiment with MilliQ water. It shows that no gas is measurably lost or acquired during the experiment.

## An automated gas exchange tank for natural seawater samples

K. Schneider-Zapp et al.

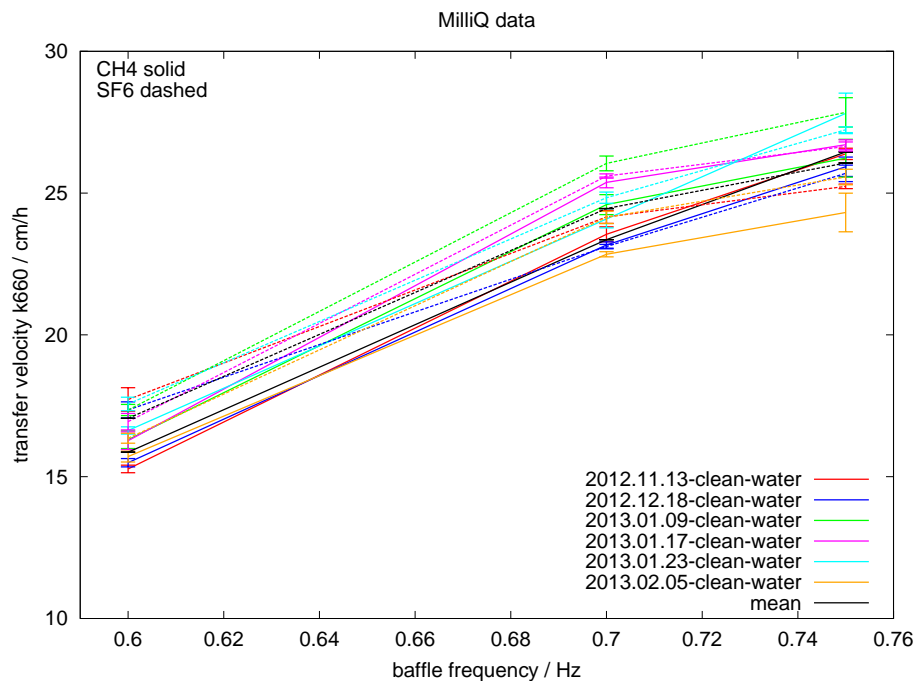


**Fig. 8.** Estimated transfer velocities of MilliQ water scaled to Schmidt number 660 at 3 different baffle settings for 6 different experiments, for both CH<sub>4</sub> and SF<sub>6</sub>.

Title Page

Abstract

Introduction

Conclusions

References

Tables

Figures

◀

▶

◀

▶

Back

Close

Full Screen / Esc

Printer-friendly Version

Interactive Discussion



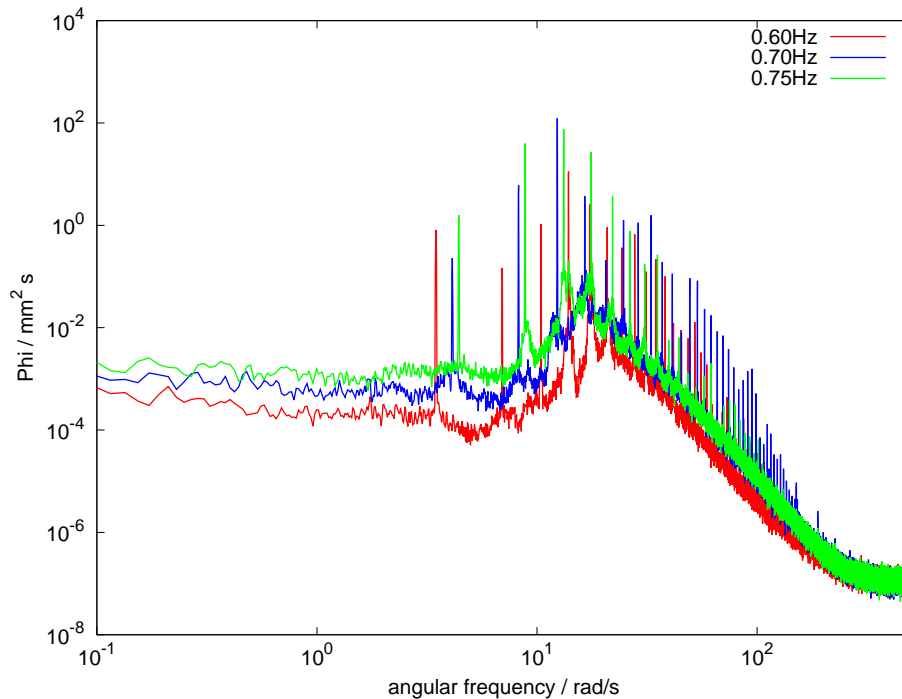


**Fig. 9.** Wave spectra of a typical gas exchange experiment with MilliQ water. The first peak for each boundary condition corresponds to the respective baffle speed, peaks at higher frequencies to harmonics.

**An automated gas exchange tank for natural seawater samples**

K. Schneider-Zapp et al.

Title Page	
Abstract	Introduction
Conclusions	References
Tables	Figures
◀	▶
◀	▶
Back	Close
Full Screen / Esc	
Printer-friendly Version	
Interactive Discussion	



## An automated gas exchange tank for natural seawater samples

K. Schneider-Zapp et al.

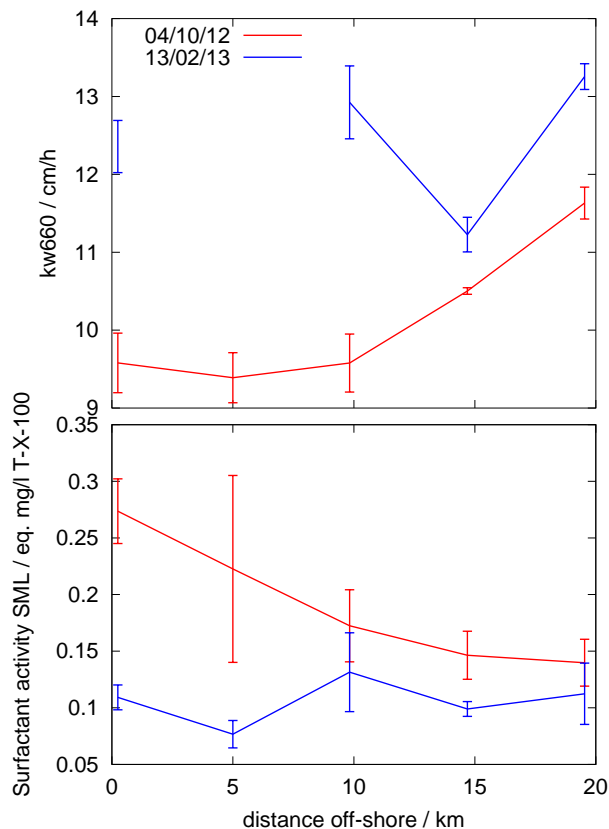


**Fig. 10.** Top: estimated transfer velocities of seawater samples scaled to Schmidt number 660 for two transects in the coastal North Sea off north-east England. Bottom: measured surfactant activity (SA) of the surface microlayer (SML) on transects in the coastal North Sea off north-east England. Results are expressed as equivalent concentration of the calibration surfactant Triton T-X-100.

